International Journal of Nanomedicine

Dovepress
open access to scientific and medical research

Open Access Full Text Article

ORIGINAL RESEARCH

Lx2-32c–loaded polymeric micelles with small size for intravenous drug delivery and their inhibitory effect on tumor growth and metastasis in clinically associated 4T1 murine breast cancer

This article was published in the following Dove Press journal:
International Journal of Nanomedicine
19 October 2016
Number of times this article has been viewed

Li-qing Chen
Wei Huang
Zhong-gao Gao
Wei-shuo Fang
Ming-ji Jin

State Key Laboratory of Bioactive Substance and Function of Natural Medicines, Institute of Materia Medica, Chinese Academy of Medical Sciences and Peking Union Medical College, Beijing, People's Republic of China

Abstract: Lx2-32c is a novel taxane derivative with a strong antitumor activity. In this study, we developed Lx2-32c–loaded polymeric micelles (Lx2-32c-PMs) with small size and investigated their antitumor efficacy against tumor growth and metastasis on 4T1 murine breast cancer cell line with Cremophor EL–based Lx2-32c solution as the control. In this study, copolymer monomethoxy polyethylene glycol$_{2000}$–polylactide$_{1300}$ was used to prepare Lx2-32c-PMs by film hydration method, and their physicochemical properties were characterized as well, according to morphology, particle size, zeta potential, in vitro drug release, and reconstitution stability. Under confocal laser scanning microscopy, it was observed that Lx2-32c-PMs could be effectively taken up by 4T1 cells in a time-dependent manner. Cell Counting Kit-8 assay showed that the IC_{50} of Lx2-32c-PMs was 0.3827 nM. Meanwhile, Lx2-32c-PMs had better ability to promote apoptosis and induce G_2/M cycle block and polyploidy formation, compared with Lx2-32c solution. More importantly, in vivo animal studies showed that compared to Lx2-32c solution, Lx2-32c-PMs possessed better ability not only to effectively inhibit the tumor growth, but also to significantly suppress spontaneous and postoperative metastasis to distant organs in 4T1 orthotopic tumor-bearing mice. Consequently, Lx2-32c-PMs have significantly prolonged the survival lifetime of tumor-bearing mice. Thus, our study reveals that Lx2-32c-PMs had favorable antitumor activity and exhibited a good prospect for application in the field of antitumor therapy.

Keywords: Lx2-32c, micelles, small size, 4T1 mammary carcinoma, tumor therapy, metastasis

Introduction

Cancer is a leading cause of death worldwide, accounting for 8.2 million deaths in 2012.[1] Breast cancer is the second leading cause of cancer death and has a high mortality. Also, breast cancer is the most common cancer among women, both in developed and developing countries. Every year, more than 500,000 women die from breast cancer around the world. In resource-poor areas, a majority of women with breast cancer are diagnosed at an advanced stage of disease, and their 5-year survival rates are low, in the range of 10%–40%.[2] Currently, the development of new therapeutic agents against cancer, especially for breast cancer, still remains an important issue.

Lx2-32c (Figure 1) is a semisynthetic taxane derivative which was obtained from the structural modification of cephalomannine by Prof Weishuo Fang in our institute; it exhibits strong antitumor activity.[3] The antitumor mechanisms of Lx2-32c include promoting microtubule polymerization, reducing the Tau-protein expression, and decreasing the pump efflux of P-glycoprotein, thus maintaining high intracellular drug concentration

Correspondence: Wei Huang; Zhong-gao Gao
State Key Laboratory of Bioactive Substance and Function of Natural Medicines, Institute of Materia Medica, Chinese Academy of Medical Sciences and Peking Union Medical College, 1 Xian Nong Tan Street, Beijing 100050, People's Republic of China
Email huangwei@imm.ac.cn; zggao@imm.ac.cn

submit your manuscript | www.dovepress.com
Dovepress
http://dx.doi.org/10.2147/IJN.S116347

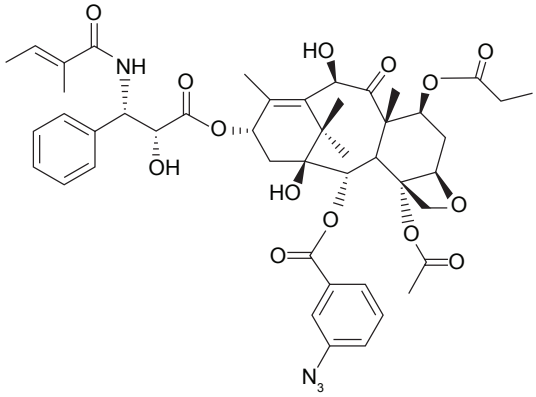

Figure 1 Chemical structure of Lx2-32c.

and inducing cell apoptosis.[4] Lx2-32c can inhibit the growth of different tumor cells in vitro, while in vivo, it also has significant inhibitory effects on Lewis lung cancer, non-small cell lung carcinoma, gastric carcinoma, and ovarian carcinoma.[5,6] However, similar to other taxane compounds, Lx2-32c is also insoluble in water, resulting in difficulty in preparing injection dosage form for intravenous (iv) delivery. Although Lx2-32c can be dissolved in a solvent mixture of Cremophor EL (polyoxyethylated castor oil) and ethanol (1:1, v/v) to prepare a conventional injection referred to as commercial Taxol®, several drawbacks are encountered in the clinical use of Cremophor EL. The most common are anaphylactic hypersensitivity reactions, hyperlipidemia, neurotoxicity, and so on. In addition, it could dissolve divinyl hexyl phthalates in the polyvinyl chloride infusion sets and alter the pharmacokinetics and pharmacodynamic profiles of paclitaxel.[7–9] Therefore, it is necessary to develop Cremophor-free drug delivery system (DDS) for iv delivery of Lx2-32c.

Recently, amphiphilic polymer micelles have drawn more attention and become popular as a DDS. Polymer micelles are a thermodynamic stability system with core–shell structure and nanoscale size formed by self-assembly in the solution. Monomethoxy polyethylene glycol-polylactide (mPEG–PLA) double-block polymer is a crucial member among all amphiphilic polymers. In mPEG–PLA polymers, PLA segments have good biocompatibility and biodegradability and their ultimate metabolites are carbon dioxide and water which can be removed fast from the body. Another segment, polyethylene glycol (PEG), is a kind of hydrophilic block used commonly with a good hydrophilicity and biocompatibility. In our previous study, we synthesized double-block polymers (block ratio 60/40) and prepared docetaxel-loaded $mPEG_{2000}$–PLA_{1300} micelles.[10] Our results indicated that such docetaxel-loaded micelles had remarkable antitumor effect in vitro and in vivo, and thus, $mPEG_{2000}$–PLA_{1300} micelles have good prospects for application in the antitumor field.

Therefore, based on the superior antitumor effect of Lx2-32c and the similarity in molecular structure between Lx2-32c and docetaxel, in this study, we employed $mPEG_{2000}$–PLA_{1300} copolymer to prepare Lx2-32c-loaded polymeric micelles (Lx2-32c-PMs) for the first time and further investigated the antitumor effect of Lx2-32c-PMs on 4T1 breast cancer in vitro and in vivo. The 4T1 mouse mammary tumor cell line is one of only a few breast cancer models having the capacity to metastasize efficiently to sites similar to human breast cancer when implanted orthotopically, and it is also a late stage breast cancer.[11,12] So, 4T1 cells were selected as the model system in the present study. Considering that there is no commercialized product of Lx2-32c, we employed Cremophor EL and ethanol (v/v =1:1) as the solvent to obtain Lx2-32c solution, referred to as Taxol®, in this study. Accordingly, the in vitro and in vivo antitumor activities of Lx2-32c-PMs were assessed in comparison to Lx2-32c solution.

Materials and methods

Materials

Double-block copolymer $mPEG_{2000}$–PLA_{1300} (molecular weight [MW] 3,300, block ratio 60/40) was synthesized in our laboratory previously.[10] Lx2-32c compound ($C_{46}H_{54}N_4O_{14}$, MW 886.36, Lot no. 32C-140114, purity 99.8%) was kindly supplied by Prof Weishuo Fang from the Department of Natural Medicinal Chemistry, Institute of Materia Medica, Chinese Academy of Medical Sciences and Peking Union Medical College. Fluorescent probe 1,1′-dioctadecyl-3,3,3′,3′-tetramethyl indotricarbocyanine iodide (DiR) fluorescent probe was obtained from Head (Beijing) Biotechnology Co., Ltd. (Beijing, People's Republic of China). Cremophor EL was purchased from BSAF Company (Ludwigshafen, Germany). Medicinal anhydrous ethanol was bought from Nanjing Chemical Reagent Co., Ltd. (Nanjing, People's Republic of China). Coumarin-6 and Hoechst 33258 were obtained from Sigma-Aldrich Co. (St Louis, MO, USA). Cell Counting Kit-8 (CCK-8) was provided by Dojindo Laboratories (Kumamoto, Japan). Annexin V-fluorescein isothiocyanate/propidium iodide (FITC/PI) apoptosis detection kit was purchased from KeyGen Biotech (Nanjing, People's Republic of China). Fetal bovine serum (FBS) was supplied by Shanghai ExCell Biology Inc. (Shanghai, People's Republic of China). Roswell Park Memorial Institute (RPMI) 1640 medium, 0.25% trypsin–0.53 mM ethylenediaminetetraacetic acid solution, and phosphate-buffered saline (PBS) were all purchased from Thermo Fisher Scientific (Walthan, MA, USA). In situ cell death detection kit-peroxidase method (POD) was supplied by Hoffman-La Roche Ltd. (Basel, Switzerland). Acetonitrile and methanol

(high performance liquid chromatography [HPLC] grade) were obtained from Sigma-Aldrich Co. All other chemicals were of analytical grade and used without further purification.

Preparation of Lx2-32c-PMs

A film hydration method was employed to prepare Lx2-32c-PMs.[13] Briefly, Lx2-32c and $mPEG_{2000}$–PLA_{1300} were dissolved in acetonitrile in a round-bottom flask to obtain a mixture. Then, the solvent acetonitrile was evaporated by rotary evaporation at 45°C for 30 minutes to get a uniform thin film. The residual solvent was removed under vacuum overnight at room temperature. Subsequently, the thin film was hydrated with water at 45°C to obtain a micelle solution. The resultant micelle solution was then filtered through a 0.22 μm microporous filtration membrane (EMD Millipore, Billerica, MA, USA). The blank micelle solution was prepared in the same manner without the drug. Ultimately, both drug-containing and blank micelle solutions were freeze-dried to obtain the final powder preparation of micelles.

Preparation of Lx2-32c solution

Lx2-32c powder was accurately weighed and dissolved in anhydrous ethanol. Then, isopycnic Cremophor EL was added to the above anhydrous ethanol to obtain about 6 mg/mL drug-containing solution. Afterward, the prepared Lx2-32c solution was sterilized by filtration through 0.22 μm microporous membrane. The actual content of Lx2-32c in the solution was measured by a reverse-phase high performance liquid chromatography (RP-HPLC) mentioned below. The final Lx2-32c solution was preserved at 4°C as standby stock.

Morphology of Lx2-32c-PMs

Morphology of Lx2-32c-PMs was observed using transmission electron microscopy (Hitachi H-7650; Hitachi Ltd., Tokyo, Japan) at 200 kV. In short, the sample solution was deposited on a carbon grid and made to stand for 5 minutes, was then sucked dry with a filter paper and negatively stained with 2% phosphotungstic acid solution for another 5 minutes. The carbon grid was left to stand for a while to be dried under infrared lamp. Finally, the carbon grid was subjected to transmission electron microscopy to observe the morphology of Lx2-32c-PMs.

Particle size and zeta potential of Lx2-32c-PMs

The particle size, polydispersity index (PDI), and zeta potential of Lx2-32c-PMs were assayed through dynamic light scattering and electrophoretic light scattering. The lyophilized Lx2-32c-PM powder was reconstituted and diluted to a concentration of 1 mg/mL with double-distilled water. Then, the measurements of particle size, PDI, and zeta potential were performed at a scattering angle of 90° using a Zetasizer Nano ZS90 (Malvern Instruments, Malvern, UK).

Reconstitution stability of Lx2-32c-PMs

The lyophilized powder of Lx2-32c-PMs was reconstituted with 5% glucose solution to obtain 5 mL Lx2-32c-PM solution at a concentration of 1 mg/mL. The reconstituted Lx2-32c-PM solution was left at room temperature. At the time points of 0, 2, and 6 hours, 1 mL of solution was taken out to measure the particle size and PDI value for evaluating the reconstitution stability of Lx2-32c-PMs.

Entrapment efficiency and loading capacity of Lx2-32c-PMs

The drug entrapment efficiency (EE%) and loading capacity (LC%) of Lx2-32c-PMs were determined through an RP-HPLC analysis system (Agilent 1200 series; Agilent Technologies, Palo Alto, CA, USA). A Diamonsil C8 column (150×4.6 mm, 5 μm) was used for the separation. Mobile phase was composed of acetonitrile–methanol–water (41:4:55), and the flow rate and column temperature were set at 1.5 mL/min and 30°C, respectively. The ultraviolet absorbance was determined at 218 nm, and the wavelength at 360 nm was set as a reference. The injection volume of the sample was 20 μL. Exactly 20.2 mg Lx2-32c drug powder was dissolved in 25 mL ethanol to get Lx2-32c stock solution at a concentration of 0.808 mg/mL. Lx2-32c stock solution was diluted with mobile phase to a series of concentrations of 16.2, 32.3, 80.8, 161.6, 242.4, and 323.2 μg/mL. All these solutions were subjected to HPLC analysis according to the above conditions. Then, a linear regression between Lx2-32c concentration (C) and peak area (A) was conducted to get a standard curve. Moreover, the RP-HPLC method was validated through evaluating the precision, accuracy, and recovery. Further, the solution of Lx2-32c-PMs (200 μL) was diluted three times using an accurate volume of ethanol. The Lx2-32c-PMs solution was subjected to ultrasound for 10 minutes and then centrifuged at 10,000 rpm for 10 minutes. Finally, the supernatant was collected to assay Lx2-32c concentration through the established HPLC method. EE% and LC% values were calculated as follows:

$$EE\% = \frac{\text{Weight of encapsulated drug}}{\text{Weight of total drug}} \times 100\%$$

$$LC\% = \frac{\text{Weight of encapsulated drug}}{\text{Weight of total drug and vector}} \times 100\%$$

In vitro release

The release profile of Lx2-32c from Lx2-32c-PMs was determined at 37°C in phosphate buffer solution (pH 7.4) as the release medium. In brief, 0.5 mL of Lx2-32c-PMs solution at a concentration of 1 mg/mL was transferred into a dialysis bag (MW cutoff: 10 kDa; MYM Biological Technology Co., Ltd., Hyderabad, India). Then, the dialysis bag was immersed in 40 mL PBS containing 0.5% (w/v) Tween-80 in a triangular flask and shaken at a speed of 100 rpm. At a specific time in the assay, 0.2 mL of release medium was taken out and replaced with 0.2 mL fresh medium. The obtained medium samples were centrifuged at 10,000 rpm for 10 minutes, and the supernatants were collected to measure Lx2-32c concentration using the above established RP-HPLC method. Finally, the amount of released Lx2-32c was calculated and the accumulation release curve plotted.

Cell line and cell culture

Mouse mammary cell line 4T1 was purchased from the Cell Culture Center of Institute of Basic Medical Sciences in Chinese Academy of Medical Sciences. Another mouse mammary cell line 4T1^{luc}, which stably expresses the firefly luciferase, was a self-constructed cell line by our lab in the previous study.[14] The 4T1 and 4T1^{luc} cell lines were cultured with RPMI 1640 medium supplemented with 10% FBS at 37°C in a humidified atmosphere containing 5% CO_2. Cells in the logarithmic growth phase were used in the following cell experiments.

Cellular uptake assay

4T1 cells were seeded into a six-well plate with coverslips on the well bottom. After incubation at 37°C for 24 hours, the culture medium in the well was replaced with fresh medium containing coumarin-6–loaded polymeric micelles (C6-PMs). At the assay time points of 1, 15, 30, and 60 minutes, the cell monolayer was rinsed three times with cold PBS to remove excess C6-PMs, and then fixed with 4% paraformaldehyde solution for 10 minutes. Then, the coverslips were taken out from the wells and put on glass slides. Ninety percent glycerol was used to seal around coverslips. Finally, the cells on coverslips were viewed and imaged at an excitation wavelength of 488 nm under a confocal laser scanning microscope (TCS-SP2; Leica Microsystems, Wetzlar, Germany).

Cell viability assay

Cell viability was measured using CCK-8 assay. Briefly, 4T1 cells were seeded in 96-well plates at a density of 4×10^4 cells/well and were cultured with RPMI 1640 medium containing 10% FBS at 37°C for 24 hours to adhere in an incubator. Then, the medium in each well was replaced with fresh medium containing a series of different test samples for another 24- or 48-hour culture. Subsequently, 20 μL of CCK-8 reagent was added to each well and the cells were incubated at 37°C for another 2 hours. Ultimately, the optical density (OD) values were measured at 490 nm with 650 nm as the reference, using a Synergy H1 Microplate Reader (BioTek Instruments, Inc., Winooski, VT, USA). Cell viability was calculated with the following formula:

$$\text{Cell viability (\%)} = \frac{OD_{test} - OD_{blank}}{OD_{control} - OD_{blank}} \times 100$$

Hoechst staining assay

Hoechst staining assay was conducted for detecting cell apoptosis qualitatively. When 4T1 cells grew to about 60% confluence, the culture medium was substituted with a fresh medium containing 5 μg/mL Lx2-32c-PMs or Lx2-32c solution and the cells were cultivated for another 24 or 48 hours. Then, the cells were fixed with 4% paraformaldehyde at 4°C for 15 minutes and washed with PBS twice. Subsequently, the cells were stained with Hoechst 33258 staining reagent at a concentration of 5 μg/mL for 10 minutes and then washed with PBS twice. After air drying, the cells were observed and photographed under IX51 inverted fluorescence microscope (Olympus Corporation, Tokyo, Japan).

Annexin V-FITC/PI double-staining assay

The percentage of apoptotic 4T1 cells was quantitatively determined by Annexin V-FITC/PI double-staining assay. 4T1 cells were seeded into a 12-well plate at a density of 7×10^4 cells/well and cultured at 37°C for 24 hours to adhere in an incubator. After treatment with a medium containing 5 μg/mL Lx2-32c-PMs or Lx2-32c solution for 48 hours, the cells were washed with PBS twice and collected for Annexin V-FITC and PI staining according to the manufacturer's protocol (KeyGen Annexin V-FITC apoptosis detection kit). After sieving through 300-mesh nylon net, the cells were analyzed by FACSAria flow cytometry (BD, Franklin Lakes, NJ, USA).

Cell cycle analysis

Cell cycle distribution was analyzed by flow cytometry. 4T1 cells were seeded into a six-well plate and incubated at 37°C for 24 hours to adhere. After incubation in a medium containing 5 μg/mL Lx2-32c-PMs or Lx2-32c solution for 24 hours, the cells were harvested and then transferred into cold 70% ethanol for 24 hours at −20°C. Then, the fixed cells were washed with PBS twice and resuspended in PBS solution containing 100 μg/mL RNase A. After treatment in a water

bath at 37°C for 30 minutes, the cells were stained with PI reagent at a final concentration of 50 μg/mL for 1 hour at room temperature. Finally, the cell cycle was assayed using FACSAria flow cytometry.

Orthotopic murine breast cancer model

Six-week-old BALB/c female mice were purchased from Beijing Vital River Laboratory Animal Technology Co., Ltd. (Beijing, People's Republic of China). This study was approved by the Institute of Materia Medica in Chinese Academy of Medical Sciences (CAMS) and Peking Union Medical College (PUMC). All animal experiments have been approved by the Laboratory Animal Ethics Committee of the Institute of Materia Medica in CAMS and PUMC. The operational procedures of animal experiments abided by national and institutional principles and protocols for the care and use of experiment animals. Mouse mammary cancer model was established through subcutaneously inoculating 1×10^5 $4T1^{luc}$ cells into the fourth mammary pad in the 6-week-old mice. When the tumor grew to the volume of interest, the tumor-bearing mice were used in the animal experiments discussed below.

Antitumor evaluation of Lx2-32c-PMs in vivo

As mentioned above, the mouse mammary cancer model was established and the tumor size was monitored every other day. When the tumor volume reached about 80 mm^3, the tumor-bearing mice were randomized into three groups (n=6) which were: 5% glucose solution group, Lx2-32c solution group, and Lx2-32c-PMs group (dose =12 mg/kg). Every 7 days, all groups were treated four times by iv injection through the tail vein. On one side, the tumor size was measured with a digital caliper and the tumor volume was calculated using the formula: volume = $a^2 \times b/2$, where a represents the minor diameter and b the major diameter.

Also bioluminescence imaging analysis was conducted to detect tumor growth and metastasis using an IVIS® Spectrum CT in vivo imaging system (Caliper Life Sciences Inc., Mountain View, CA, USA), and the observation images were obtained and processed through Living Image® software (version 4.3.1; Caliper Life Sciences Inc.). In brief, at the time points used for imaging, mice were injected intraperitoneally with the substrate D-luciferin at a dose of 150 mg/kg and then anesthetized with isoflurane. After 17 minutes, the mice were placed in the imaging chamber and bioluminescence signal was acquired for 1 minute with an *F*-value of 2 and a binning value of 4.

At the end of the experiment, the mice were quickly killed by cervical dislocation, 14 minutes after injecting D-luciferin, and tissues (liver, heart, spleen, lung, kidney, and tumor) were harvested for ex vivo imaging. The bioluminescence strength was quantified as total flux (photons/s) in a region of interest. Subsequently, all lung tissues were immersed in Bouin's fixative solution for 16 hours and then were washed with 50% ethanol and photographed. All tumor tissues were weighed for quantitative comparison. Furthermore, the lung tissues were fixed with 4% neutral buffered formaldehyde, paraffin embedded, and stained with hematoxylin and eosin (H&E). The H&E-stained lung tissues were subjected to histopathological characterization, and the tissue slides were photographed under a light microscope (DM4000B; Leica Microsystems). Also, apoptosis in tumor tissue was detected by terminal-deoxynucleotidyl transferase mediated nick end labeling (TUNEL) assay using a TUNEL-POD kit according to the manufacturer's protocol.

Postoperative antimetastatic activity of Lx2-32c-PMs in vivo

In order to evaluate the postoperative antimetastatic activity of Lx2-32c-PMs in vivo, we established the model of postoperative chemotherapy. Firstly, mouse mammary cancer model was established as mentioned above and the tumor size was monitored every other day. When the tumor size reached about 6 mm, the tumor was excised entirely through surgery operation. After 10 days, these mice were randomized into three groups (n=6) which were: 5% glucose solution group, Lx2-32c solution group, and Lx2-32c-PMs group (dose =12 mg/kg). Every 7 days, all groups were treated three times by iv injection through the tail vein. After 4 months, the mice were killed by cervical dislocation and tissues were harvested for histopathological characterization.

Survival analysis

Twenty 4T1 tumor-bearing mice were randomly divided into three groups (n=6) which were: 5% glucose solution group, Lx2-32c solution group, and Lx2-32c-PMs group (dose =10 mg/kg). Every 7 days, all groups were treated three times by iv injection through the tail vein. The day on which 4T1 cells were inoculated in mice was considered as the beginning time point, and the mice were monitored for 53 days on a daily basis until they died. Survival curves were plotted according to the Kaplan–Meier method using GraphPad Prism software (version 5.0.0.0; GraphPad Software Inc., San Diego, CA, USA).

Statistical analysis

The release curve of Lx2-32c-PMs was fitted by Matlab software (version 7.0.0; The MathWorks Inc.,

Natick, MA, USA) and DDSolver software (version 1.0).[15] Representative results are presented and expressed as mean ± standard deviation (SD). Statistical analysis was conducted using SPSS 19 (version 4.0.100.1124; IBM Corporation, Armonk, NY, USA). Statistical comparisons were performed to determine group differences through analysis of variance. Significant difference between two groups was evaluated by Student's *t*-test. Asterisks indicate statistical significance as follows: $*P<0.05$, $**P<0.01$, $***P<0.001$.

Results and discussion

Preparation and physicochemical characterization of Lx2-32c-PMs

In recent years, polymeric micelles have shown good prospects for application as drug carriers due to their favorable solubilization capacity and extended biologic half-life of the hydrophobic drug.[16] Especially, the mPEG–PLA copolymer, a popular kind of material, has gained worldwide interest as a DDS. The stability of taxanes in mPEG–PLA micelles is associated with the block ratio of mPEG and PLA segments. Previous studies have shown that mPEG–PLA with 60/40 block ratio was suitable to load taxanes with good stability.[10,17] So, we chose $mPEG_{2000}$–PLA_{1300} with 60/40 block ratio to encapsulate Lx2-32c for preparing micelles. In preliminary experiments, we measured the critical micelle concentration of $mPEG_{2000}$–PLA_{1300} which gave a value of 4.677 μg/mL, indicating that the $mPEG_{2000}$–PLA_{1300} polymer was thermodynamically stable and resistant to blood dilution. Through the film hydration method, the polymer $mPEG_{2000}$–PLA_{1300} could encapsulate hydrophobic Lx2-32c to form Lx2-32c-PMs suspension with a transparent and homogeneous appearance. It was found that Lx2-32c-PMs exhibited sphere-like shape with almost uniform size under transmission electron microscopy (Figure 2A). Further assay results showed that Lx2-32c-PMs had an average particle size of 24.65±0.21 nm and a narrow particle distribution with a PDI value of 0.135±0.03 (Figure 2B), which was consistent with the above results. Also, Lx2-32c-PMs had a negative zeta potential of –9.67±1.32 mV (Figure 2C), and this suggests that Lx2-32c-PMs particles are negatively charged, which ensures the dispersion stability of Lx2-32c-PMs due to the mutual repulsion effect of charge among micelles.

In order to determine the content of Lx2-32c, we established an HPLC quantitative method. The results showed that there was a good linear relationship between Lx2-32c peak area (A) and Lx2-32c concentration (C) in the range of 16.2–323.2 μg/mL. The standard curve equation was as follows: $A = 27.256 \times C - 36.611$ ($R^2=0.9999$, n=5). Also, this HPLC method was validated through evaluation of precision, accuracy, and recovery, which suggested that it was suitable for the accurate quantitation of Lx2-32c. Subsequently, the assay results showed that the EE% and LC% of Lx2-32c-PMs were 95.80%±0.10% and 16.0%±0.15%, respectively. Our results suggested that Lx2-32c–loaded $mPEG_{2000}$–PLA_{1300} micelles exhibited good stability and LC% of Lx2-32c, which confirmed that the $mPEG_{2000}$–PLA_{1300} micelle is a good delivery vector for Lx2-32c. The good stability of Lx2-32c–loaded $mPEG_{2000}$–PLA_{1300} micelles may be attributed to the good compatibility with Lx2-32c, higher viscosity, and poor fluidity of PLA in micellar core, so as to make Lx2-32c dissolve and maintain certain stability in the PLA core.[18]

Genexol-PM® (mPEG–b-PLA/paclitaxel), manufactured by Korean Samyang Company (Seoul, Republic of Korea), is the world's first nanoscale micelle preparation and it came to market in 2006. As we all know, Genexol-PM is supposed to be diluted with 500 mL of 5% glucose solution and infused iv for 3 hours, in clinical use.[19,20] So, the reconstituted Lx2-32c-PMs should keep stable for at least 3 hours in vitro at room temperature. Therefore, in this study, the lyophilized Lx2-32c-PM preparation was also reconstituted with 5% glucose solution and the reconstitution stability was checked for 6 hours at room temperature through detecting changes in average particle size and PDI value. Also, in order to investigate the reconstitution problem of lyophilized Lx2-32c-PMs without any cryoprotectant, we did not add any lyoprotectant in the freeze-drying process in this study. The results showed that these two indexes did not remarkably change compared to those of Lx2-32c-PMs prior to lyophilization, and the average particle size and PDI value of Lx2-32c-PM reconstitution solution remained stable for 6 hours (Figure 2D and E), which suggested that the freeze-drying operation had no significant influence on Lx2-32c-PMs and that the reconstitution stability of Lx2-32c-PMs was fine and met the requirements of iv administration.

In vitro drug release profile of Lx2-32c-PMs

To characterize the drug release profile, Lx2-32c-PMs were put into a dialysis bag and incubated in release medium with gentle shaking at 37°C. The accumulation drug release curve is shown in Figure 2F. It was found that Lx2-32c released fast in the first 2 hours and then slowly in the later 70 hours, and the drug accumulation release percentage reached over 65% after 72 hours. Furthermore, six release models were used to mathematically fit the drug release curve through Matlab and DDsolver software. The fitted results are listed in Table 1.

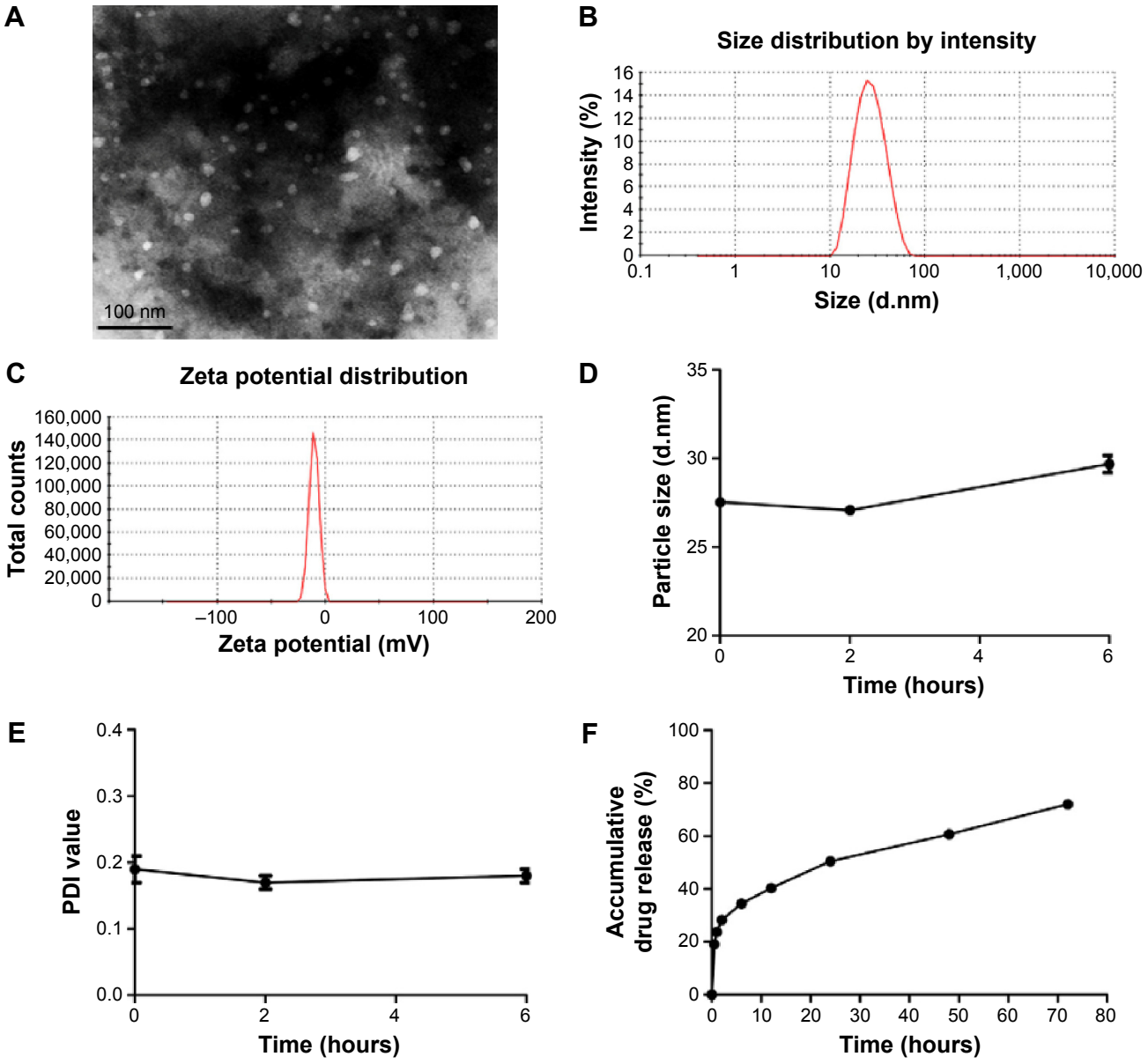

Figure 2 Physicochemical characterization of Lx2-32c-PMs.
Notes: (**A**) TEM image (magnification ×53000). (**B**) Size distribution. (**C**) Zeta potential. (**D**) Particle size and (**E**) PDI changes over time after reconstitution with 5% glucose solution. (**F**) In vitro release profile of Lx2-32c-PMs in PBS (pH 7.4) at 37°C.
Abbreviations: Lx2-32c-PMs, Lx2-32c–loaded polymeric micelles; PBS, phosphate-buffered saline; PDI, polydispersity index; TEM, transmission electron microscopy.

Table 1 Fit result of in vitro release of Lx2-32c-PMs

Release model	Equation	Fit result	Fit (R^2)
Zero order	F=F0+kt	Q=22.294+0.776t	0.7978
First order	F=Fmax*{1−Exp[−k*(t−m)]}	F=68.126*{1−Exp[−0.056*(t+4.515)]}	0.8993
Higuchi	F=F0+kt^0.5	F=12.875+7.267t^0.5	0.9382
Ambiexponent equation	F=F0−(Ae^αt+Be^βt)	F=0.9912−[0.3372e^−0.9082t+0.6783e^−0.01251t]	0.9800
Korsmeyer–Peppas	F=k*t^n	F=22.056*t^0.267	0.9936
Peppas–Sahlin	F=k1*t^m+k2*t^(2*m)	F=17.081*t^0.202+5.223*t^(2*0.202)	0.9954
Weibull	F=100*{1−Exp[−(t^β)/α]}	F=100*{1−Exp[−(t^0.357)/4.153]}	0.9838

Note: In the table, the symbols * and ^ represent multiply and exponential power, respectively.
Abbreviation: Lx2-32c-PMs, Lx2-32c–loaded polymeric micelles.

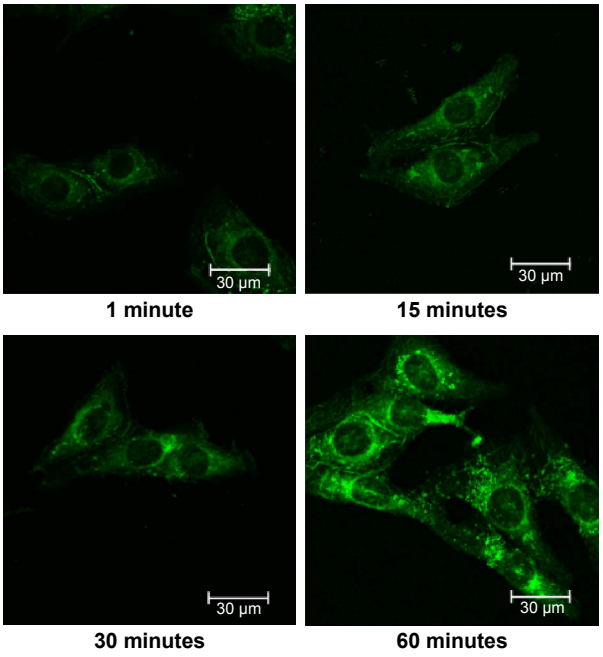

Figure 3 Confocal microscopic images of 4T1 cells after incubation with C6-PMs for 1, 15, 30, and 60 minutes, respectively (scale bar =30 μm), magnification ×400.
Abbreviation: C6-PMs, coumarin-6–loaded polymeric micelles.

The results suggested that the drug release behavior of Lx2-32c-PMs conformed to the Peppas–Sahlin sustained-release model due to the highest R^2 value of 0.9954 (Table 1).

Cellular uptake assay

The fluorescent probe coumarin-6 was physically encapsulated into micelles to prepare C6-PMs for investigating the intracellular uptake of micelles in 4T1 cells. The results of confocal laser scanning microscopy are presented in Figure 3. It is observed that the green fluorescence signal could be detected at 1 minute postincubation with C6-PMs and gradually becomes stronger with extended incubation time, and that C6-PMs are mainly distributed in the cytoplasm. This suggests that micelles could be quickly taken up by 4T1 cells with a high efficiency, which ensures that Lx2-32c-PMs could deliver Lx2-32c to cells.

Cytotoxicity of blank PMs

The cytotoxicity of blank micelles and blank solution was evaluated by CCK-8 assay. Compared with the conventional MTT assay, CCK-8 assay is characterized by high sensitivity, good reproducibility, easy and simple handling, and so on. The results of cytotoxicity assay against 4T1 cells are shown in Figure 4A. It was found that viabilities of all cells were higher than 85% within all tested equivalent concentrations of Lx2-32c ranging from 0.0005 to 50 μg/mL. This suggested that blank PMs did not exhibit significant cytotoxicity, and they possessed good safety and biocompatibility as a drug delivery carrier. However, the blank solution itself showed strong inhibition of 4T1 cells in a time-dependent and dose-dependent manner. Consequently, when the cells were cultured with 0.05 and 0.5 μg/mL of Lx2-32c for 24 hours, there still existed significant difference between Lx2-32c-PMs and Lx2-32c solution, while it was not found when the cells were incubated for 48 hours (Figure 4B). Cytotoxicity of Cremophor EL was confirmed in doxorubicin-resistant human breast cancer cell lines and various human tumor samples.[21–23] It was postulated that formation of free radicals

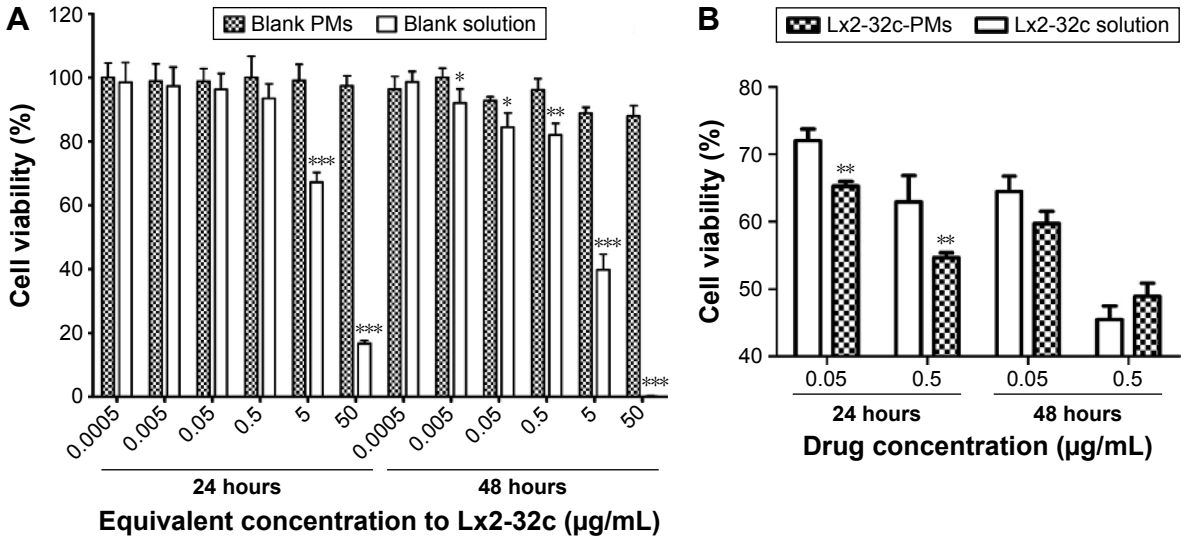

Figure 4 (**A**) Cytotoxicity of blank PMs and blank solution after incubation for 24 and 48 hours (n=4, mean ± SD); *$P<0.05$ versus blank PMs, **$P<0.01$ versus blank PMs, ***$P<0.001$ versus blank PMs. (**B**) Cell viability comparison between Lx2-32c-PMs and Lx2-32c solution after incubation for 24 and 48 hours (n=4, mean ± SD); **$P<0.01$ versus Lx2-32c solution.
Abbreviations: PMs, polymeric micelles; SD, standard deviation.

by peroxidation of polyunsaturated fatty acids and/or a direct perturbing effect in the cell membrane causing fluidity and leakage are the possible mechanisms contributing to this type of cytotoxicity.[24–26] In addition, considering that 4T1 cells grow rapidly, cytotoxicity of Cremophor EL should be more obvious compared to control cells in control wells.

Inhibitory effect of Lx2-32c-PMs on 4T1 cell proliferation

In view of the strong inhibitory effect of the blank solution, it was hard to say what contributed to proliferative inhibition in Lx2-32c solution. So, in this study, we only evaluated the inhibitory capacity of Lx2-32c-PMs against 4T1 cell proliferation by CCK-8 assay. The results are shown in Figure 5A. It was found that Lx2-32c-PMs could effectively inhibit the proliferation of 4T1 cells in a dose-dependent pattern in the concentration range of 0.0005–50 μg/mL for 48 hours. The IC_{50} of Lx2-32c-PMs on 4T1 cells was only 0.3268 μg/mL (0.3827 nM). As we can see in Figure 5B, 4T1 cells grew rapidly, and possessed fine extensibility and flat shape under normal culture conditions. After treating 4T1 cells with Lx2-32c-PMs, compared to normal cells in the control group, cells in Lx2-32c-PMs group grew slowly with a significant reduction of cell quantity and there were many apoptotic or dead cells (bright and spherical). In addition, the cell size increased and the cell morphology became irregular. These changes reflected effective inhibition of Lx2-32c-PMs on 4T1 cells' proliferation.

Influence of Lx2-32c-PMs on cell apoptosis and cell cycle

The previous study showed that Lx2-32c could enhance microtubule polymerization and induce bundling of microtubules as well as multinucleation in a pattern similar to that of paclitaxel.[27] Cells treated with Lx2-32c manifested apoptosis, G_2/M phase arrest, and numerical chromosome abnormality.[4] In this study, similar results have been obtained. Hoechst staining assay (Figure 6) showed that in treated groups, nuclear morphological changes are found with typical apoptotic features such as chromatin condensation, nuclear fragmentation, and chromosome abnormality. It was found that the perinuclear apoptotic bodies and multinucleated cells appeared posttreatment with Lx2-32c-PMs or Lx2-32c solution. The quantification of apoptotic cells and G_2/M cycle arrest ratio were further investigated through Annexin V-FITC/PI double-staining assay and PI staining assay by flow cytometry. As presented in Figure 6A, the cycle arrest results show that Lx2-32c could arrest 4T1 cell cycle at G_2/M phase and subsequently induce polyploidy formation after 24 hours of treatment. The total ratio of cells at G_2/M and polyploidy phase (M2+M3) was 61.90% in Lx2-32c-PMs group, while it was 50.29% in Lx2-32c solution group. As shown in Figure 6B, after treatment for 48 hours, Lx2-32c mainly induced late cellular apoptosis (upper right quadrant) of 4T1 cells. The late apoptotic cell ratio in Lx2-32c-PMs was 44.09%±0.79%, which was significantly higher than that in Lx2-32c solution group (38.78%±0.89%) (**$P<0.01$). Generally, it was confirmed that Lx2-32c-PMs could effectively deliver and release Lx2-32c to arrest 4T1 cell cycle at G_2/M and induce apoptosis, and sequentially inhibit cell proliferation. Also, we can now explain the cell morphology changes posttreatment with Lx2-32c-PMs as shown in Figure 5B. These changes were the consequence of cell apoptosis and cell cycle arrest induced by Lx2-32c-PMs.

In vivo antitumor effect of Lx2-32c-PMs

The in vivo antitumor efficacy of Lx2-32c-PMs against murine breast cancer was investigated to explore the antitumor

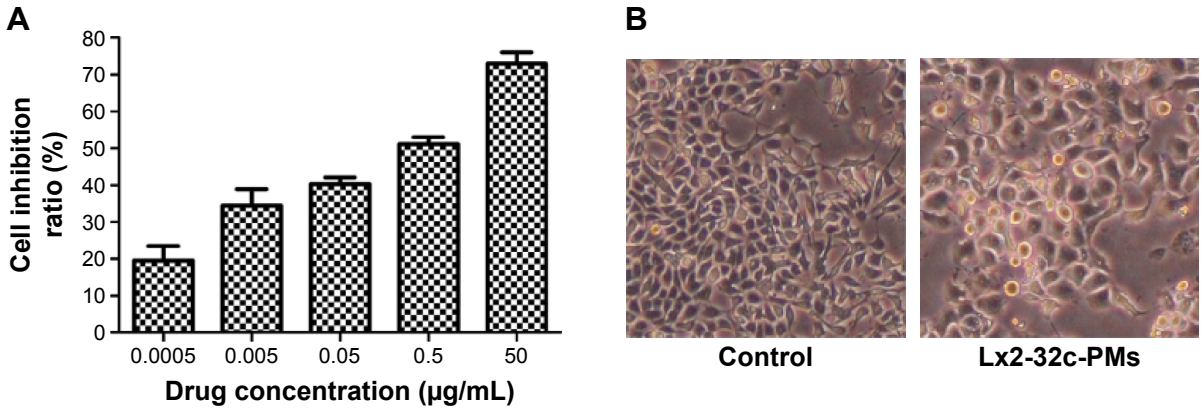

Figure 5 (**A**) Inhibitory effect of Lx2-32c-PMs on 4T1 cell proliferation after incubation for 48 hours (n=4, mean ± SD). (**B**) Cellular morphology changes observed under microscope after treatment with Lx2-32c-PMs (magnification ×100).
Abbreviations: Lx2-32c-PMs, Lx2-32c–loaded polymeric micelles; SD, standard deviation.

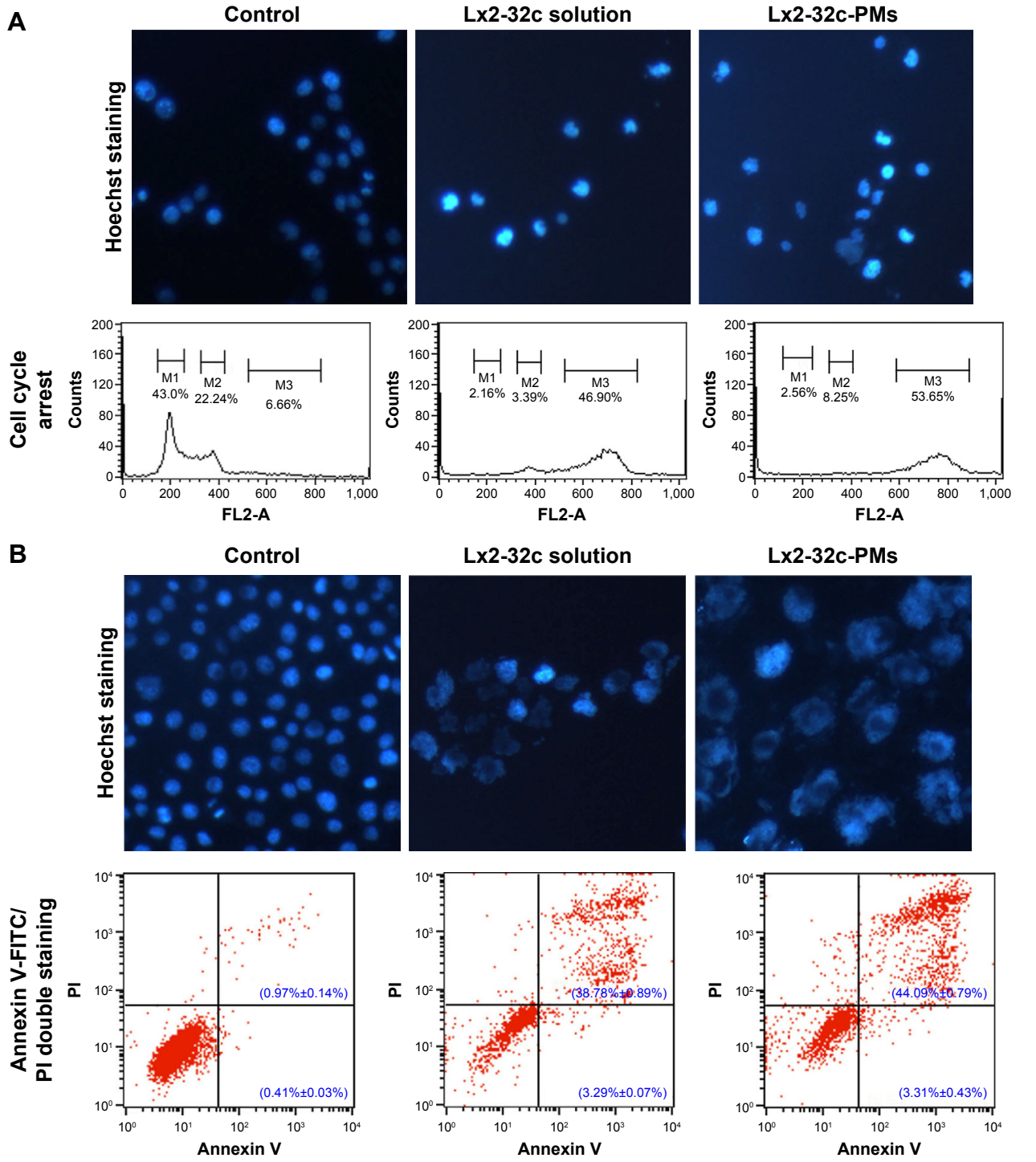

Figure 6 Apoptosis and cycle arrest caused by Lx2-32c-PMs.
Notes: (**A**) Hoechst staining (magnification ×200) and the corresponding cycle arrest assay after 24-hour incubation. M1, G_0/G_1 phase; M2, G_2/M phase; M3, polyploidy. (**B**) Hoechst staining (magnification ×200) and the corresponding Annexin V-FITC/PI staining assay after 48-hour incubation.
Abbreviations: Lx2-32c-PMs, Lx2-32c–loaded polymeric micelles; FITC, fluorescein isothiocyanate; PI, propidium iodide.

potential of Lx2-32c-PMs. The $4T1^{luc}$ cells were inoculated into female BALB/c mice to construct a murine breast cancer model. Once the tumor volume reached about 80 mm^3, Lx2-32c-PMs, Lx2-32c solution, and 5% glucose solution as negative control were, respectively, administered to tumor-bearing mice for antitumor therapy. In order to monitor the tumor growth, the tumor volumes at various time points were measured with vernier caliper, and bioluminescence imaging detection in vivo was performed at the same time. Bioluminescence imaging was able to reveal the real-time

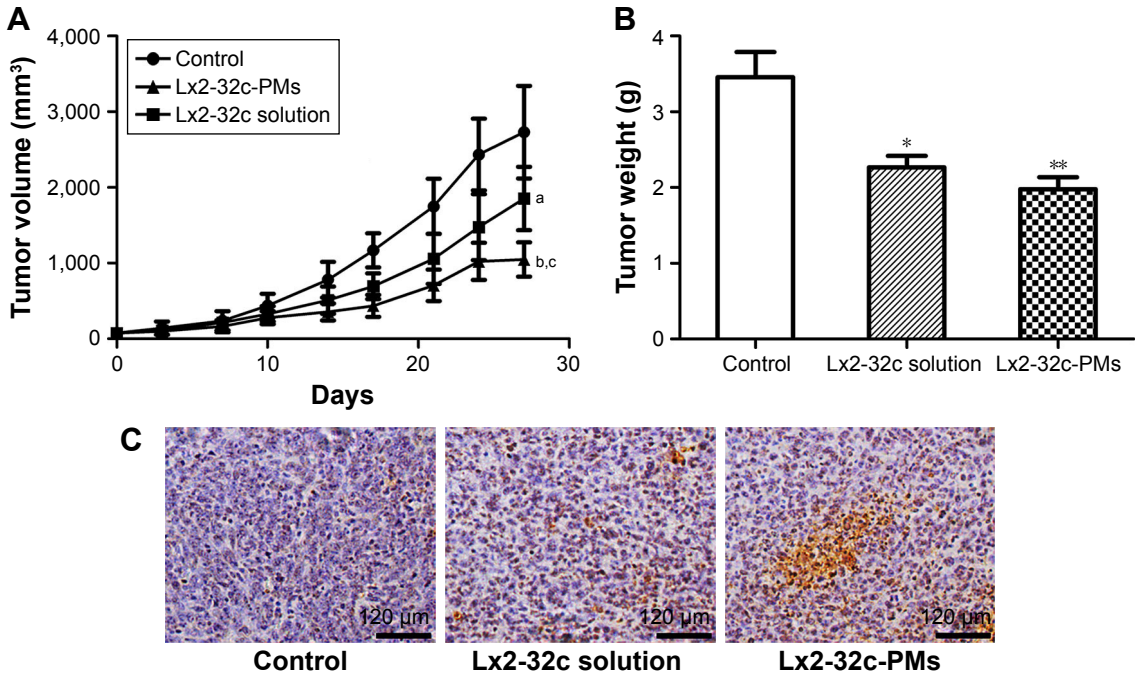

Figure 7 In vivo antitumor activity of Lx2-32c-PMs injected intravenously through the tail vein in 4T1 tumor-bearing Balb/c mice.
Notes: (**A**) Tumor volume changes in mice during the experiment; data are expressed as mean ± SD (n=6); $^{a}P<0.05$, $^{b}P<0.001$ versus the control, $^{c}P<0.01$ versus Lx2-32c solution. (**B**) Tumor weight calculated 27 days postinjection with 5% glucose solution, Lx2-32c solution, and Lx2-32c-PMs injected through tail veins; data are expressed as mean ± SD (n=3); $*P<0.05$, $**P<0.01$ versus the control group. (**C**) Paraffn-embedded tumor sections after TUNEL (the apoptotic cells are shown in brown), scale bar =120 μm, magnification ×200.
Abbreviations: Lx2-32c-PMs, Lx2-32c–loaded polymeric micelles; SD, standard deviation; TUNEL, terminal-deoxynucleoitidyl transferase mediated nick end labeling.

tumor growth and metastasis over time. The results of tumor volume showed that the tumors of mice in the control group grew rapidly, but the tumors in Lx2-32c-PMs group and Lx2-32c solution group grew slowly (Figure 7A). Moreover, tumor volume in Lx2-32c-PMs group at the final checking point was significantly smaller than that in Lx2-32c solution group. In addition, the results of in vivo imaging detection showed that the bioluminescence intensity of tumor in Lx2-32c-PMs group increased slowly in contrast to that in Lx2-32c solution group (Figure 8A and B), which was consistent with the results of tumor volume given above. After the final monitoring of tumor volume and bioluminescence intensity, mice were sacrificed to compare the tumor weights. The results showed that the average tumor weight in Lx2-32c-PMs group and Lx2-32c solution group was significantly lower than that in control group ($**P<0.01$ and $*P<0.05$, respectively) (Figure 7B). Also, TUNEL assay was carried out to detect apoptosis or necrosis in tumor tissues. The results are shown in Figure 7C. Tumor cell quantity decreased in both Lx2-32c-PMs group and Lx2-32c solution group. More TUNEL-positive cells (brown) were found in Lx2-32c-PMs group than in Lx2-32c solution group, and this suggested that Lx2-32c-PMs could effectively accumulate and deliver Lx2-32c to the tumor sites and release Lx2-32c to induce cell apoptosis in the tumor tissue and further inhibit the growth of tumor.

Inhibition of spontaneous metastasis and postoperative metastasis by Lx2-32c-PMs

We firstly studied inhibition of spontaneous metastatic activity by Lx2-32c-PMs. We know that spontaneous metastasis usually occurs in late stages of cancer, and 4T1, a representative of metastasis, primarily metastasizes to the lung.[11] Likewise, ex vivo imaging (Figure 8C) revealed that bioluminescence signal could be detected in the lung (yellow arrow) of control group, which revealed that many tumor cells were most likely to metastasize to lungs. In order to confirm this, we dissected lung tissues from mice and fixed them with Bouin's solution to observe tumor metastasis to lungs. We could clearly see many white nodules (red arrow) on the surfaces of lung lobes in the control group and a few of them in the Lx2-32c solution group, while almost no nodules were observed on the surfaces of lungs in the Lx2-32c-PMs group (Figure 8D). It has been reported that the appearance of nodules is an indicator of tumor lung metastasis.[28] This evidence was further confirmed by H&E staining. As illustrated in Figure 8D, there existed a huge tumor metastasis locus (red dotted circle) in the lung of control group and a smaller one in the lung of Lx2-32c group, while there was none in the lung of Lx2-32c-PMs group. In addition, edema, hypertrophic lung interval, and reduced alveolar structure were severe in the lungs of control group and Lx2-32c solution

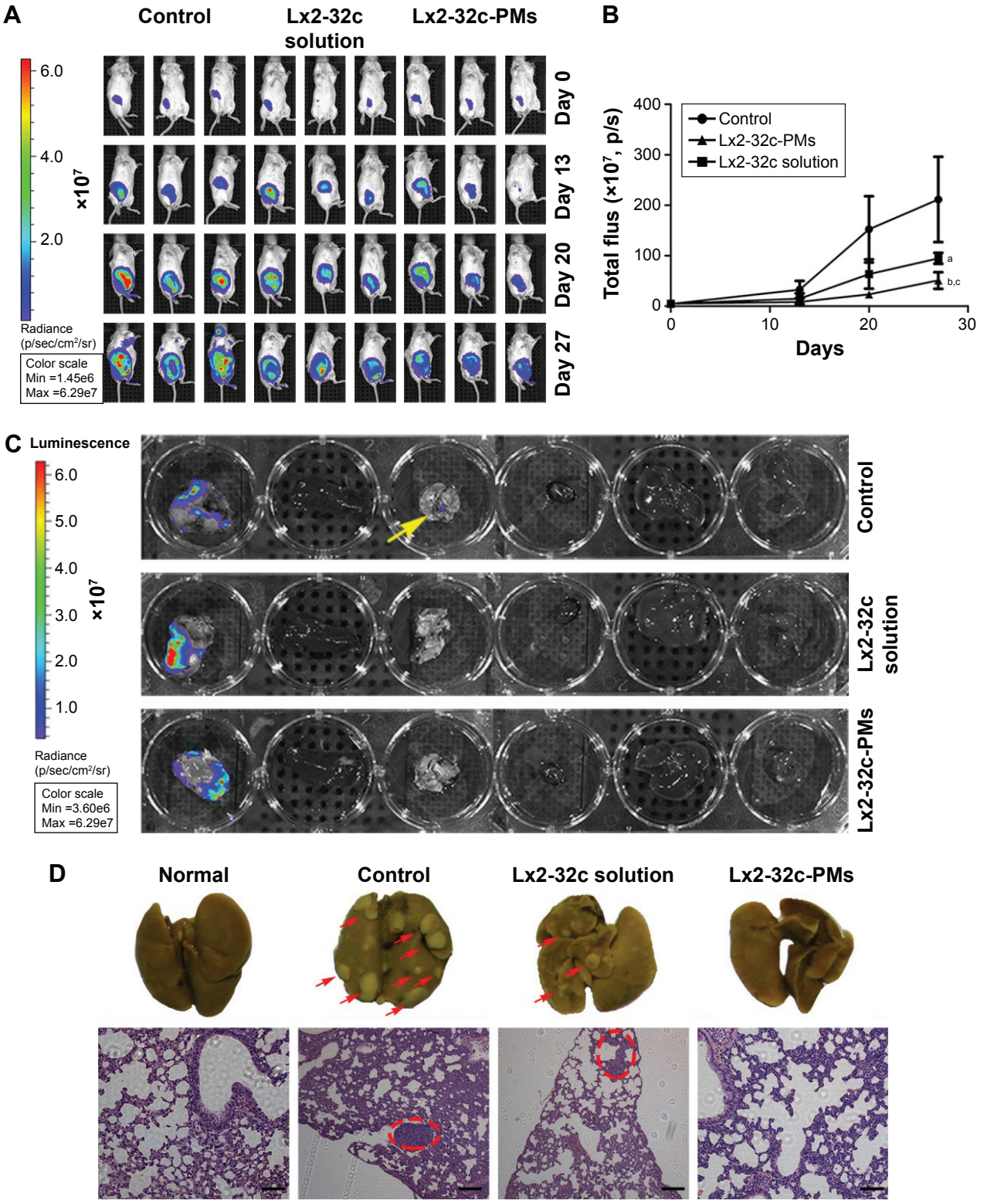

Figure 8 (**A**) Typical bioluminescence images of tumor growth over time according to groups. Mice are imaged at 0, 13, 20, and 27 days postadministration. (**B**) Comparison of in situ bioluminescence intensity values between groups; data are expressed as mean ± SD (n=3); $^{a}P<0.01$, $^{b}P<0.01$ versus the control, $^{c}P<0.05$ versus Lx2-32c solution. (**C**) Typical bioluminescence images of the organs dissected from mice 27 days postadministration. (**D**) Representative images of lungs and corresponding H&E staining in spontaneous metastasis models, scale bar =120 μm, magnification ×100.

Notes: Yellow arrow shows the bioluminescence signal detected in the lung tissue of the control group. Red arrows indicate the white nodules on the surfaces of lung lobes. Red dotted circles show the tumor metastasis loci in the lungs.

Abbreviations: H&E, hematoxylin and eosin; Lx2-32c-PMs, Lx2-32c–loaded polymeric micelles; SD, standard deviation; Min, minimum; Max, maximum.

group, while these phenomena were not obvious in the lung of Lx2-32c-PMs group. In conclusion, the above results suggested that Lx2-32c-PMs exhibited stronger ability to inhibit tumor metastasis to lungs than Lx2-32c solution.

In clinical situations, surgery is frequently employed to remove primary mammary tumors, but approximately 33% of women successfully treated for primary tumors still die subsequently due to metastatic disease.[14] Thus, in order to evaluate the postoperative antimetastatic activity of Lx2-32c-PMs in vivo, primary 4T1 tumors were removed surgically to simulate the metastatic disease in an animal setting. The results of pathological examination of lung and liver tissues are presented in Figure 9. In the control group and Lx2-32c solution group, significant tumor micrometastasis (yellow arrow) was observed in the liver, while there was none in the Lx2-32c-PMs group. Although no significant tumor micrometastasis was observed in the lungs of the three groups, vascular extravasation of tumor cells (yellow arrow) was still obvious in the control group and Lx2-32c solution group. However, vascular extravasation was mild in Lx2-32c-PMs group. These results were consistent with a previous report that breast cancer could metastasize to distant organs through a hematogenous route.[29] Also, we found that inflammatory cell (neutrophils, yellow dotted circle) invasion was remarkable in the control group. As we know, inflammation is associated with cancer metastasis.[30] Moreover, bleeding, edema, hypertrophic lung interval, and reduced alveolar structure were more obvious in the control group and Lx2-32c solution group than in Lx2-32c-PMs group. These results demonstrate that Lx2-32c-PMs could effectively inhibit postoperative metastases of the tumor to remote organs.

Studies have shown that about 90% of cancer patients die of tumor invasion and metastasis.[31] Despite the remarkable progress achieved in breast cancer screening and early diagnosis over the past 3 decades, approximately 5%–6% of all breast cancer patients in the US and Western Europe have distant metastases at the initial presentation.[32,33] The median survival rate of females with metastatic breast cancer is only 2–3 years.[34] Current nanotechnologies focus on eliminating primary tumors based on enhanced penetration and retention in well-vascularized primary tumors.[35] However, size of a tumor clone after secondary metastasis is generally less than 100 mm^3. Tumor angiogenesis is not obvious and blood perfusion is poor. Therefore, enhanced penetration and retention effect fails for metastasis loci.[36] In addition, lymph node metastasis is one of the major pathways for tumor formation and it is difficult to deliver enough chemotherapeutics to lymph node metastasis for various reasons.[37] Although the affected lymph nodes can be removed by surgery, tumor cells remain inside the lymphatic vessels.[38] The strategy of using small-sized nanocarriers to promote penetration into poorly vascularized tumors and the lymph system has drawn much attention recently.[39,40] Cabral et al compared the accumulation and effectiveness of different sizes of long circulating, drug-loaded polymeric micelles (with diameters of 30, 50, 70, and 100 nm) in both highly and poorly permeable tumors.[39] They found that only 30 nm micelles could penetrate poorly permeable pancreatic tumors to achieve an antitumor effect, and that the penetration and efficacy of the larger micelles could be enhanced by using a transforming growth factor-β inhibitor to increase the permeability of the tumors. Meanwhile, Reddy et al found that 25 nm nanoparticles could be transported highly efficiently into lymphatic capillaries and their draining lymph nodes, compared with 100 nm nanoparticles.[40] In this study, the mean diameter of Lx2-32c-PMs was about 25 nm. Likewise, Lx2-32-PMs belong to the small-size DDS, and thus, we speculated that Lx2-32c-PMs can improve penetration into the lymph system and poorly perfused distal metastasis loci of breast cancer, which may be one of the mechanisms that explain the superior antimetastatic efficacy of Lx2-32c-PMs. But the molecular basis underlying its inhibitory functions remains obscure and further experiments are needed to address this issue.

Influence of Lx2-32c-PMs on survival time of tumor-bearing mice

Based on the effective inhibition effect on tumor growth and metastasis which has been confirmed above, we further evaluated the influence of Lx2-32c-PMs on the survival time of 4T1 tumor-bearing mice. As seen in Figure 10, the log-rank analysis showed that Lx2-32c solution group prolonged the median survival to 44 days versus 37 days for the control group (**$P<0.01$). In contrast, Lx2-32c-PMs group significantly prolonged the average survival time to 50 days (***$P<0.001$ vs control). So, it was demonstrated that Lx2-32c-PMs could remarkably prolong the survival time of 4T1 tumor-bearing mice.

It is well known that triple-negative breast cancer (TNBC) accounts for about 10%–17% of all invasive breast cancers.[41] TNBC is characterized by the lack of estrogen receptor (ER), progesterone receptor (PR), and human epidermal growth factor receptor 2 (HER2) in cancer cells; it has poor prognosis,[42] increased likelihood of distant recurrence, and high mortality.[41–44] As of now, limited therapeutic agents are

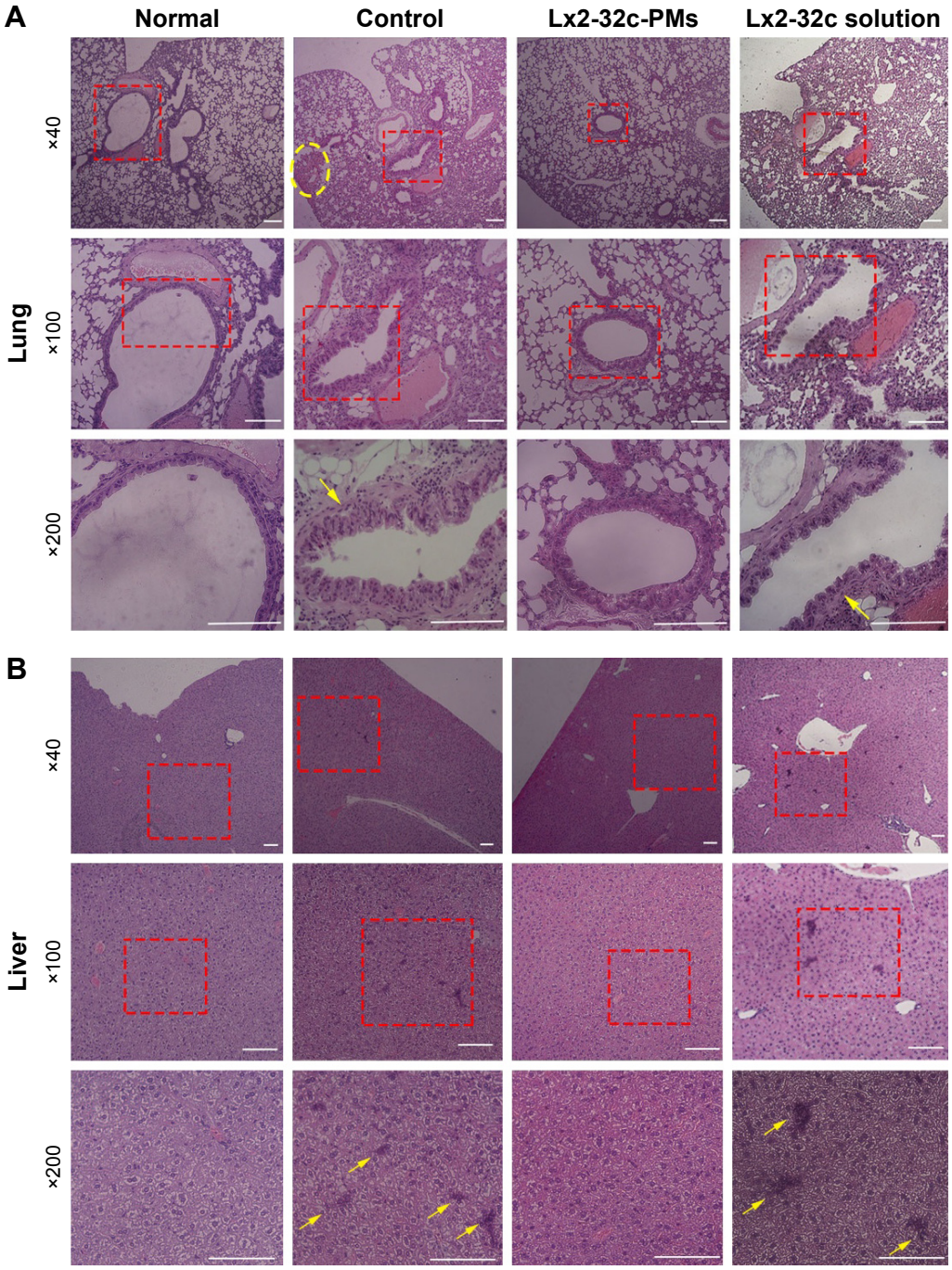

Figure 9 Postoperative antimetastatic activity of Lx2-32c-PMs.
Notes: (**A**) Paraffn-embedded lung sections after H&E staining in postoperative metastasis models, scale bar =100 μm. (**B**) Paraffin-embedded liver sections after H&E staining in postoperative metastasis models, scale bar =100 μm. Yellow arrows indicate vascular extravasation of tumor cells in H&E-stained images of lung or micrometastasis loci in H&E-stained images of liver. Red dotted boxes denote further amplification areas. Yellow dotted circle indicates neutrophils' invasion in lungs.
Abbreviations: H&E, hematoxylin and eosin; Lx2-32c-PMs, Lx2-32c–loaded polymeric micelles.

available for TNBC in the late phase. Also, TNBC patients cannot benefit from the popular HER2-targeted monoclonal antibodies in clinical use. It has been reported that 4T1 cell line is characterized as ER–/PR–/HER2– and its growth and metastasis to many distant organs including the lungs, liver, bone, and brain are very similar to those of human breast cancer cells.[45–48] So, 4T1 murine breast cancer is a representative model of TNBC. In this respect, our results suggested that Lx2-32c-PMs could also serve as a therapeutic agent for TNBC.

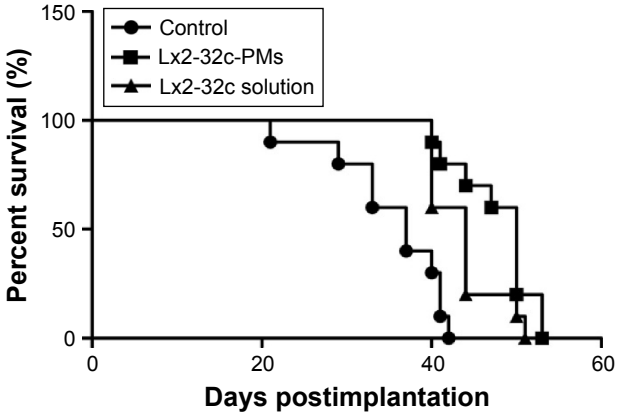

Figure 10 Kaplan–Meier survival curves of 4T1 tumor-bearing Balb/c mice.
Notes: $P<0.001$, Lx2-32c-PMs versus the control; $P<0.01$, Lx2-32c solution versus the control.

Conclusion

In summary, we have developed small-sized Lx2-32c-PMs with good physicochemical properties and also evaluated their antitumor activity in vitro and in vivo using the clinically relevant 4T1 murine breast cancer model. Compared with Lx2-32c solution, Lx2-32c-PMs demonstrated more effective impact on the proliferation, G_2/M cycle arrest, and apoptosis of 4T1 cancer cells in vitro. More importantly, Lx2-32c-PMs significantly inhibited tumor growth and metastasis, and thus prolonged the survival life time of 4T1 tumor-bearing mice. Thus, Lx2-32c-PMs may be used in the treatment of orthotopic breast cancer or in postoperative chemotherapy. In future, Lx2-32c-PMs will be thoroughly investigated according to the drug registration regulations, which would enable us to ultimately develop them into a novel antitumor agent for clinical use.

Acknowledgments

This work was financially supported by National Natural Science Foundation of China (81373342), Beijing Natural Science Foundation (2141004, 7142114), and Basic Research Special Foundation for Central Public Service Research Institutes (2014ZD02).

Disclosure

The authors report no conflicts of interest in this work.

References

1. World Health Organization Data [homepage on the Internet]. Geneva: NCD mortality and morbidity. Available from: http://www.who.int/gho/ncd/mortality_morbidity/en/. Accessed June 29, 2016.
2. World Health Organization Programmes [homepage on the Internet]. Geneva: WHO position paper on mammography screening. Available from: http://www.who.int/cancer/publications/mammography_screening/en/. Accessed June 29, 2016.
3. Xiao X, Wu J, Trigili C, et al. Effects of C7 substitutions in a high affinity microtubule-binding taxane on antitumor activity and drug transport. *Bioorg Med Chem Lett*. 2011;21(16):4852–4856.
4. Zhou Q. Studies on anti-drug-resistance activities and mechanisms of action of Lx2-32c, a novel taxane [dissertation]. Beijing: Chinese academy of medical sciences & Peking union medical college; 2012.
5. Wang HB, Li HY, Zuo MX, et al. Lx2-32c, a novel taxane and its antitumor activities in vitro and in vivo. *Cancer Lett*. 2008;268(1):89–97.
6. Wang HB, Li HY, Fang WS, Chen XG. Inhibiting effect of Lx2-32c, one taxane derivant, on the proliferation of human ovary A2780 cells. *Chin New Drug J*. 2008;17(10):833–836.
7. Gelderblom H, Verweij J, Nooter K, Sparreboom A. Cremophor EL: the drawbacks and advantages of vehicle selection for drug formulation. *Eur J Cancer*. 2001;37(13):1590–1598.
8. Waugh WN, Trissel LA, Stella VJ. Stability, compatibility, and plasticizer extraction of taxol (NSC-125973) injection diluted in infusion solutions and stored in various containers. *Am J Hosp Pharm*. 1991;48(7):1520–1524.
9. van Zuylen L, Karlsson MO, Verweij J, et al. Pharmacokinetic modeling of paclitaxel encapsulation in Cremophor EL micelles. *Cancer Chemother Pharmacol*. 2001;47(4):309–318.
10. Li YF, Yang FF, Chen W, et al. A novel monomethoxy polyethylene glycol-polylactic acid polymeric micelles with higher loading Capacity for docetaxel and well reconstitution characteristics and its antimetastasis study. *Chem Pharm Bull*. 2012;60(9):1146–1154.
11. Kaur P, Nagaraja GM, Zheng H, et al. A mouse model for triple-negative breast cancer tumor-initiating cells (TNBC-TICs) exhibits similar aggressive phenotype to the human disease. *BMC Cancer*. 2012;12:120.
12. Tao K, Fang M, Alroy J, Sahagian GG. Imagable 4T1 model for the study of late stage breast cancer. *BMC Cancer*. 2008;8:228.
13. Gaucher G, Dufresne MH, Sant VP, Kang N, Maysinger D, Leroux JC. Block copolymer micelles: preparation, characterization and application in drug delivery. *J Controll Release*. 2005;109(1–3):169–188.
14. Li YF, Jin Jin MJ, Shao S, et al. Small-sized polymeric micelles incorporating docetaxel suppress distant metastases in the clinically-relevant 4T1 mouse breast cancer model. *BMC Cancer*. 2014;14:329.
15. Zhang Y, Huo MR, Zhou JP, et al. DD Solver: an add-in program for modeling and comparison of drug dissolution profiles. *AAPS J*. 2010;12(3):263–271.
16. Mikhail AS, Allen C. Block copolymer micelles for delivery of cancer therapy: transport at the whole body, tissue and cellular levels. *J Controll Release*. 2009;138(3):214–223.
17. Zhang XC, Jackson JK, Burt HM. Development of amphiphilic diblock copolymers as micellar carriers of taxol. *Int J Pharm*. 1996;132(1):195–206.
18. Burt HM, Zhang XC, Toleikis P, Embree L, Hunter WL. Development of copolymers of poly(d,l-lactide) and methoxypolyethylene glycol as micellar carriers of paclitaxel. *Colloids Surf B Biointerfaces*. 1999;16(1–4):161–171.
19. Kim TY, Kim DW, Chung JY, et al. Phase I and pharmacokinetic study of Genexol-PM, a cremophor-free, polymeric micelle-formulated paclitaxel, in patients with advanced malignancies. *Clin Cancer Res*. 2004;10(11):3708–3716.
20. Lee KS, Chung HC, Im SA, et al. Multicenter phase II trial of Genexol-PM, a Cremophor-free, polymeric micelle formulation of paclitaxel, in patients with metastatic breast cancer. *Breast Cancer Res Treat*. 2008;108(2):241–250.
21. Fjällskog ML, Frii L, Bergh J. Is Cremophor EL, solvent for paclitaxel, cytotoxic? *Lancet*. 1993;342(8875):873.
22. Nygren P, Csoka K, Jonsson B, et al. The cytotoxic activity of Taxol in primary cultures of tumour cells from patients is partly mediated by CremophorEL. *Br J Cancer*. 1995;71(3):478–481.

23. Csóka K, Dhar S, Fridborg H, Larsson R, Nygren P. Differential activity of Cremophor EL and paclitaxel in patients' tumor cells and human carcinoma cell lines in vitro. *Cancer*. 1997;79(6):1225–1233.
24. Bégin ME, Ells G, Horrobin DF. Polyunsaturated fatty acid-induced cytotoxicity aganist tumor cells and its relationship to lipid peroxidation. *J Natl Cancer Inst*. 1988;80(3):188–194.
25. Siegel I, Liu TL, Yaghoubzadeh E, Keskey TS, Gleicher N. Cytotoxic effects of free acids on ascites tumor cells. *J Natl Cancer Inst*. 1987; 78(2):271–277.
26. Burton AF. Oncolytic effects of fatty acids in mice and rats. *Am J Clin Nutr*. 1991;53(Suppl 4):S1082–S1086.
27. Zhou Q, Li Y, Jin J, et al. Lx2-32c, a novel taxane derivative, exerts anti-resistance activity by initiating intrinsic apoptosis pathway in vitro and inhibits the growth of resistant tumor in vivo. *Biol Pharm Bull*. 2012;35(12):2170–2179.
28. Dan ZL, Cao HQ, He XY, et al. A pH-responsive host-guest nanosystem loading succinobucol suppresses lung metastasis of breast cancer. *Theranostics*. 2016;6(3):435–445.
29. Kang SA, Hasan N, Mann AP, et al. Blocking the adhesion cascade at the premetastatic niche for prevention of breast cancer metastasis. *Mol Ther*. 2015;23(6):1044–1054.
30. Quail DF, Joyce JA. Microenvironmental regulation of tumor progression and metastasis. *Nat Med*. 2013;19(11):1423–1437.
31. Gupta GP, Massagué J. Cancer metastasis: building a framework. *Cell*. 2006;127(4):679–695.
32. Ly BH, Nguyen NP, Vinh-Hung V, Rapiti E, Vlastos G. Loco-regional treatment in metastatic breast cancer patients: Is there a survival benefit? *Breast Cancer Res Treat*. 2010;119(3):537–545.
33. Criscitiello C, Giuliano M, Curigliano G, et al. Surgery of the primary tumor in de novo metastatic breast cancer: to do or not to do? *Eur J Surg Oncol*. 2015;41(10):1288–1292.
34. Rahman M, Mohammed S. Breast cancer metastasis and the lymphatic system. *Oncol Lett*. 2015;10(3):1233–1239.
35. Fang J, Nakamura H, Maeda H. The EPR effect: unique features of tumor blood vessels for drug delivery, factors involved, and limitations and augmentation of the effect. *Adv Drug Deliv Rev*. 2011;63(3): 136–151.
36. Schroeder A, Heller DA, Winslow MM, et al. Treating metastatic cancer with nanotechnology. *Nat Rev Cancer*. 2011;12(1):39–50.
37. Li X, Dong Q, Yan Z, et al. MPEG-DSPE polymeric micelle for translymphatic chemotherapy of lymph node metastasis. *Int J Pharm*. 2015;487(1–2):8–16.
38. Tammela T, Saaristo A, Holopainen T, et al. Photodynamic ablation of lymphatic vessels and intralymphatic cancer cells prevents metastasis. *Sci Transl Med*. 2011;3(69):69ra11.
39. Cabral H, Matsumoto Y, Mizuno K, et al. Accumulation of sub-100 nm polymeric micelles in poorly permeable tumours depends on size. *Nat Nanotechnol*. 2011;6(12):815–823.
40. Reddy ST, van der Vlies AJ, Simeoni E, et al. Exploiting lymphatic transport and complement activation in nanoparticle vaccines. *Nat Biotechnol*. 2007;25(10):1159–1164.
41. Bonzanini M, Morelli L, Bonandini EM, Leonardi E, Pertile R, Dalla Palma P. Cytologic features of triple-negative breast carcinoma. *Cancer Cytopathol*. 2012;120(6):401–409.
42. Fayaz MS, El-Sherify MS, El-Basmy A, et al. Clinicopathological features and prognosis of triple negative breast cancer in Kuwait: a comparative/perspective analysis. *Rep Pract Oncol Radiother*. 2013; 19(3):173–181.
43. Dent R, Trudeau M, Pritchard KI, et al Triple-negative breast cancer: clinical features and patterns of recurrence. *Clin Cancer Res*. 2007; 13(15):4429–4434.
44. Caldarella A, Crocetti E, Bianchi S, et al. Female breast cancer status according to ER, PR and H&ER2 expression: a population based analysis. *Pathol Oncol Res*. 2011;17(3):753–758.
45. Anders CK, Deal AM, Miller CR, et al. The prognostic contribution of clinical breast cancer subtype, age and race among patients with breast cancer brain metastases. *Cancer*. 2011;117(8):1602–1611.
46. Mi ZY, Guo HT, Wai PY, Gao CJ, Wei JP, Kuo PC. Differential osteopontin expression in phenotypically distinct subclones of murine breast cancer cells mediates metastatic behavior. *J Biol Chem*. 2004; 279(45):46659–46667.
47. Aslakson CJ, Miller FR. Selective events in the metastatic process defined by analysis of the sequential dissemination of subpopulations of a mouse mammary tumor. *Cancer Res*. 1992;52(6):1399–1405.
48. Pulaski BA, Ostrand-Rosenberg S. Reduction of established spontaneous mammary carcinoma metastases following immunotherapy with major histocompatibility complex class II and B7.1 cell-based tumor vaccines. *Cancer Res*. 1998;58(7):1486–1493.